LM-06K009
February 16, 2006

Triple-axis X-ray Reciprocal Space Mapping of $In_yGa_{1-y}As$ Thermophotovoltaic Diodes Grown on (100) InP Substrates

M Dashiell, H Ehsani, P Sander, F Newman, C Wang,
Z Shellenbarger, D Donetski, N Gu and S Anikeev

Triple-axis X-ray Reciprocal Space Mapping of $In_yGa_{1-y}As$ Thermophotovoltaic Diodes Grown on (100) InP Substrates.

M.W. Dashiell, H. Ehsani, P.C. Sander
Lockheed Martin Corporation, Schenectady, NY 12301-1072
F.D. Newman
Emcore Corporation, Albuquerque, NM 87123
C.A. Wang
MIT Lincoln Laboratory, Lexington, MA 02420
Z. A. Shellenbarger
Sarnoff Corporation, Princeton NJ, 08543-5300
D. Donetski, N. Gu, S. Anikeev
Department of Electrical Engineering, State University of New York, Stony Brook, NY 11794-2350

Abstract

Analysis of the composition, strain-relaxation, layer-tilt, and the crystalline quality of $In_yGa_{1-y}As/InP_{1-x}As_x$ thermophotovoltaic (TPV) diodes grown by metal organic vapor phase epitaxy (MOVPE) is demonstrated using triple-axis x-ray reciprocal space mapping techniques. $In_{0.53}Ga_{0.47}As$ (E_{gap}=0.74eV) n/p junction diodes are grown lattice matched (LM) to InP substrates and lattice mismatched (LMM) $In_{0.67}Ga_{0.33}As$ (E_{gap}=0.6eV) TPV diodes are grown on three-step $InP_{1-x}As_x$ ($0 < x < 0.32$) buffer layers on InP substrates. X-ray reciprocal space maps about the symmetric (**400**) and asymmetric (**533**) reciprocal lattice points (RELPs) determine the in-plane and out-of-plane lattice parameters and strain of the $In_yGa_{1-y}As$ TPV active layer and underlying $InP_{1-x}As_x$ buffers. Triple-axis x-ray rocking curves about the LMM $In_{0.67}Ga_{0.33}As$ RELP show an order of magnitude increase of its full width at half maximum (FWHM) compared to that from the LM $In_{0.53}Ga_{0.47}As$ (250asec vs. 30asec). Despite the significant RELP broadening the photovoltaic figure of merits show that the electronic quality of the LMM $In_{0.67}Ga_{0.33}As$ approaches that of the lattice matched diode material. This indicates that misfit-related crystalline imperfections are not dominating the photovoltaic response of the optimized LMM $In_{0.67}Ga_{0.33}As$ material compared with the intrinsic recombination processes and/or recombination through native point defects which would be present in both LMM and LM diode material. However, additional RELP broadening in non-optimized LMM $In_{0.67}Ga_{0.33}As$ n/p junction diodes does correspond to significant degradation of TPV diode open circuit voltage and minority carrier lifetime demonstrating that there is correlation between x-ray FWHM and the electronic performance of the LMM TPV diodes.

1.0 Introduction

Greater than 20% conversion efficiency of radiant heat energy into electricity was demonstrated with 0.6eV $In_{0.67}Ga_{0.33}As$ thermophotovoltaic (TPV) diodes employing 3-step $InP_{1-x}As_x$ buffers grown by MOVPE [1]. The TPV diode is one of the critical components of a TPV energy conversion system and its maximum electrical power (P_{max}) is the product of three parameters: the open circuit voltage (V_{OC}), the fill factor (FF) and the short circuit current (I_{SC}) [2]. The primary diode material properties which optimize these three electrical parameters for a given thermal radiation spectrum are the semiconductor bandgap (E_{gap}) and the electronic material quality. An alloy's bandgap is determined from previously established empirical relationships linking E_{gap} and alloy composition ($0 \leq x,y \leq 1$) to the values of the lattice parameters measured by x-ray diffraction. High-resolution x-ray diffraction (HRXRD) reciprocal space mapping (RSM) directly measures the in-plane and out-of-plane lattice parameters, strain, and the diffuse x-ray scattering from multilayered semiconductor heterostructures [3-4]. The technique was recently used to characterize strain-relaxation in linear and step-graded $InP_{1-x}As_x$ and $In_{1-z}Al_zAs$ buffers grown by molecular beam epitaxy (MBE) [5-7]. Diffusely scattered x-ray intensity around reciprocal lattice point (RELP) maxima results from structural imperfections [4] that can potentially degrade the diode's electronic material quality and photovoltaic response due to defect assisted minority carrier recombination. In this work, TPV diode epitaxial layers, both lattice-matched (LM) $In_{0.53}Ga_{0.47}As$ and lattice-mismatched (LMM) $In_{0.67}Ga_{0.33}As$ were grown by MOVPE and their structural characteristic were evaluated from triple axis HRXRD measurements. Analysis of the RELP maxima provide the strain, composition, and the tilt for each of the TPV layers. Evaluation of RELP broadening will be shown to be a useful tool to evaluate the electronic material quality in LMM $In_{0.67}Ga_{0.33}As$ TPV diode epitaxial layers.

2.0 Growth and fabrication of lattice matched (LM) 0.74eV $In_{0.53}Ga_{0.47}As$ and lattice mismatched (LMM) $In_{0.67}Ga_{0.33}As$ TPV Diodes.

Lattice matched 0.74eV $In_{0.53}Ga_{0.47}As$ TPV n/p junction diodes were grown on p^+ (100) InP substrates that were intentionally misoriented 2° towards the [1$\bar{1}$0] direction. The layers were

grown in a VEECO D-125 rotating-disc MOVPE reactor. The growth temperature was 600°C and the reactor pressure was 60Torr. Group III and V sources were trimethylindium, triethylgallium, tertiarybutylarsine, and tertiarybutylphosphine. Diethylzinc and diisopropyltellurium were used for p-type and n-type dopant sources respectively. Prior to growing the active $In_{0.53}Ga_{0.47}As$ epitaxial layers, a thin p^+ InP layer was grown on the InP substrate as a buffer layer and for minority carrier confinement at the p-type $In_{0.53}Ga_{0.47}As$ base. The thin n^+ $In_{0.53}Ga_{0.47}As$ emitter layer was capped with an epitaxial n^+ InP minority carrier confinement (window) layer which also served as a front contact layer. After growth, $0.5cm^2$ TPV diodes were fabricated by forming ohmic metal contact to the p^+ InP substrate and a metal grid contact was made to the n^+ InP window layer.

Lattice mismatched 0.6eV $In_{0.67}Ga_{0.33}As$ TPV n/p junction diodes were grown on (100) InP substrates that were intentionally misoriented 2° towards the [1$\bar{1}$0] in an VEECO D-180 MOVPE reactor [1,8,9]. A three-step $InP_{1-x}As_x$ buffer ($0 \le x \le 0.32$) was used to accommodate the ~1% lattice mismatch between the $In_{0.67}Ga_{0.33}As$ active region and the InP substrate [8,9]. Thin p^+ and n^+ $InP_{0.68}As_{0.32}$ layers were used for minority carrier confinement at the p-type base and n-type emitter respectively. A series of experiments were performed with equivalent epitaxial growth conditions except zinc-doped, tellurium-doped, and undoped $InP_{1-x}As_x$ buffers were used. Metal contacts were made to either conducting InP substrates for $0.5cm^2$ diodes or a heavily doped n^+ InPAs buffer which acts as a lateral conduction layer for $4cm^2$ monolithically interconnected module TPV devices [10]. In both cases a metal grid contact was made to a n^+ $In_{0.67}Ga_{0.33}As$ front contact layer.

3.0 Reciprocal Space Mapping (RSM)

Reciprocal space maps (RSMs) were used to examine the composition, strain relaxation, lattice parameters and crystalline quality of $In_yGa_{1-y}As$ TPV diode layer structures grown on InP substrates. A Bede D1 high-resolution x-ray diffractometer operating in triple-axis mode was used for all RSM and rocking curve measurements. The incident x-ray beam was conditioned using a combination (i) multilayer superlattice (tradename = MaxFlux Optic) mirror and (ii) a germanium (**220**) two-bounce crystal monochromator. The detector arm (third-axis) employs a two-bounce silicon (220) analyzer crystal for high-resolution scanning in 2Θ. The x-ray system

response was capable of resolving x-ray peak full widths at half maximum (FWHM) of 8 arcsec or greater.

In this report, the notation for diffractometer angular coordinates is that which was established in reference [4]. Reciprocal lattice point (RELP) coordinates are derived from the Ewald sphere construction and diffractometer angular positions ω and 2Θ [4,5]. For (100) oriented samples with the diffraction plane parallel to the [011] and [100] crystalline direction, the symmetric and asymmetric RELP coordinates are given by their vector components b_{l00} and b_{0hh}. The vector b_{l00} is parallel with [100] and b_{0hh} is parallel to the [011] crystallographic direction. The measured RSMs presented in this work show the epitaxial layers' (**hkl**) RELP coordinates *relative* to those of the InP substrate (**hkl**) RELPs and are labeled as Δb_{l00} and Δb_{0hh} respectively. The RSMs from LM samples were constructed from approximately three-hundred triple-axis ω-2Θ scans (5 asec steps) for ω-offsets spaced 3 asec apart around the (**400**) and (**533**) InP substrate RELPs. The RSMs from LMM samples were constructed from three hundred high resolution ω-2Θ scans (10 arc sec steps) at ω-offsets spaced 10 arc sec apart around the (**400**) and (**533**) InP substrate RELPs. Triple-axis rocking curves were measured by locating the optimized (2Θ) position of the $In_yGa_{1-y}As$ RELP maximum and then rocking the sample in the ω-scan direction in increments of 2asec.

4.0 Lattice Matched (LM) 0.74eV $In_{0.53}Ga_{0.47}As$ TPV

Figures 1a and 1b shows the symmetric (**400**) and asymmetric (**533**) RSM from a MOVPE grown 0.74eV $In_{0.53}Ga_{0.47}As$ TPV diode structure. The (**400**) $In_{0.53}Ga_{0.47}As$ RELP lies nearly coincidental to the (**400**) InP substrate RELP, indicative of near lattice matching. Pendellosung (thickness) fringes originate from the x-ray interference from the ~200nm thick InP window layer grown on top of the $In_{0.53}Ga_{0.47}As$ active region. Due to the 2° misorientation of the InP (100) crystal plane from the surface by 2° towards [$1\bar{1}0$], the line connecting the Pendellosung fringes is inclined by a small angle with respect to the $\Delta b_{110}=0$ line in the (**400**) map [11]. The low intensity analyzer streak is an experimental artifact caused by the finite size of the reciprocal space probe. The glancing-exit (**533**) asymmetric RSM shown in Fig. 1b provide reciprocal lattice vector components related directly to both the in-plane and out-of-plane lattice parameters. The large Bragg angles and high (**hkl**) Miller indices of the (**533**)

planes enable greater sensitivity to strain than the more commonly investigated (**400, 224**, and/or **115**) crystal planes [4-7]. Because of the higher Miller indices, the measured RSM shown in Fig. 1b resolves the InP substrate RELP from the $In_{0.53}Ga_{0.47}As$ RELP in the (**533**) map. Both the substrate and layer RELP maxima lie along the vertical $\Delta b_{033}=0$ line in reciprocal space, indicating that the $In_{0.53}Ga_{0.47}As$ in-plane lattice constant is coherent with that of the InP substrate (i.e. the layer is pseudomorphic). The (**533**) $In_{0.53}Ga_{0.47}As$ RELP lies below that of the substrate along the b_{500} direction indicating a compressive layer strain due to an total misfit of $\varepsilon_{misfit}=0.017\%$ with respect to the InP substrate. Absolute values of the $In_{0.53}Ga_{0.47}As$ RELP are calculated by using the InP RELP as an internal standard and assuming the InP substrate is unstrained with a lattice constant of $a_{InP}=0.58688$nm corresponding to reciprocal lattice coordinates $b_{033}^{InP} = 7229\mu m^{-1}$ and $b_{500}^{InP} = 11173\mu m^{-1}$. The absolute values of the epitaxial layers' RELP coordinates are then determined by adding the measured relative coordinates to the substrate coordinates $b_{hkl}^{Epilayer}=b_{hkl}^{InP}+\Delta b_{hkl}$. The in-plane ($a_p$) and out-of-plane ($a_n$) lattice constants of the epitaxial layer are determined from the (**533**) RELP coordinates using equation (1):

$$b_{033}^{Epilayer} = \left(\frac{3^2 + 3^2}{a_p^{\,2}} \right)^{1/2} \text{ and } b_{500}^{Epilayer} = \left(\frac{5^2}{a_n^{\,2}} \right)^{1/2} \qquad (1)$$

The relaxed lattice constant a_r of the epitaxial layer is then calculated by assuming a linear interpolation (Vegard's law) between the lattice constants and elastic coefficients of the binary alloy's constituents [12]. The $In_{0.53}Ga_{0.47}As$ lattice parameters, layer relaxation, and composition calculated from the measured RSMs are included in Table I.

RELP intensity broadening along the direction perpendicular to the diffraction vector is observed along the [**O11**] direction in Fig. 1a (in diffractometer units this corresponds to a triple axis rocking-curve or ω-scan). The $In_{0.53}Ga_{0.47}As$ (**400**) rocking curve full width at half maximum (FWHM) is $FWHM_{400}=30$asec compared with a $FWHM_{400}$ of 10asec measured from the pure InP substrate prior to MOVPE growth. Broadening of a x-ray rocking curve is typically assigned to either (i) mosaic spreading due to structural imperfections in the crystal (ii) bending of the wafer due to a change in the radius of curvature due to layer strain or (iii) strain induced tilt of a lattice matched epitaxial layer on InP substrate. Because the layer is grown coherently with the InP substrate (i.e. the layer has not relaxed via misfit dislocations) the broadening of the

$In_{0.53}Ga_{0.47}As$ FWHM is attributed to strain-induced effects rather than mosaic spreading. The observation of the low intensity diffraction patterns in Fig 1 (i.e. Pendellösung fringes and analyzer streaks) are additional indicators of high crystalline perfection and low density of misfit related defects. An increase in the InP $FWHM_{400}$ to ~20asec on the backs of InP wafers following epitaxial growth also suggests that strain/thermal effects are influencing the LM $In_{0.53}Ga_{0.47}As$ rocking curve $FWHM_{400}$.

5.0 Lattice Mismatched (LMM) 0.60eV $In_{0.67}Ga_{0.33}As$ TPV Diodes

(a) Reciprocal Space Maps

The symmetric (**400**) triple-axis RSM from representative high efficiency 0.6eV TPV diode material [1] is shown in Figure 2. The (**400**) RSM exhibits five distinct RELP maxima. The peak assignments correspond to those RELP maxima from the InP substrate (1), the first $InP_{0.85}As_{0.15}$ buffer layer (2), the second $InP_{0.73}As_{0.27}$ buffer layer (3), the third $InP_{0.68}As_{0.32}$ buffer layer (4) and the 0.6eV $In_{0.67}Ga_{0.33}As$ active region (5). The layer assignments were confirmed via selective etching of the topmost layers followed by re-measuring the RSM of remaining layers. The $In_{0.67}Ga_{0.33}As$ RELP is elongated in the [011]direction, corresponding to a rocking curve $FWHM_{400}$ of 250asec, which is an order of magnitude broader than that of the LM 0.74eV $In_{0.53}Ga_{0.47}As$ TPV shown in Figure 1a. The broadening of the LMM $In_{0.67}Ga_{0.33}As$ RELP is attributed to the mosaic nature of the epitaxial material, discussed for a number of other mismatched material systems such as InGaAs/GaAs and SiGe/Si [3-5,11]. A second feature observed in the (**400**) RSM of Fig. 2 is that the RELP maxima from all three $InP_{1-y}As_y$ buffers and the $In_{0.67}Ga_{0.33}As$ active region are not centered on the $\Delta b_{110}=0$ line, indicating that each layer possesses a net average crystallographic tilt with respect to the InP substrate. Because the InP substrate RELP is used as an internal standard, the strain analysis requires that the measured symmetrical and asymmetrical layer RELPs shown in Figs 2 and 3 must be corrected for the amount of layer tilt which is projected along the [011] crystalline direction. Therefore each epitaxial layer RELP must be rotated about the (**000**) reciprocal space origin by an angle Ω_{tilt}^{layer}, so that the symmetrical layer RELPs lie underneath the InP substrate RELP along the [**100**] direction [4]. The tilt corrected (**400**) RELPs of each layer are shown as the circles in Figure 2.

Figures 3a and 3b show the asymmetric glancing incidence (**533**) and glancing exit (**533**) RSMs of the diode sample shown in Figure 2. Layer peak assignments are labeled the same as for Figure 2. For strain analysis, the measured (**533**) layer RELPs must be rotated about the (**000**) origin by the angle $\pm\Omega_{tilt}^{layer}$ which was determined from the (**400**) RSM: these are shown as the tilt corrected RELPs (circles) in Fig 3a and Fig 3b. Strain and compositional analysis, as described in Section IV, is then performed on each tilt-corrected (**533**) RELPs in either the glancing incidence or glancing exit geometry. The magnitude of in-plane and out-of-plane lattice constants of the epitaxial layers are determined from each of the tilt-corrected (**533**) asymmetric RELP positions in reciprocal space using equation (1). Epitaxial layer lattice parameters and InAs content of each layer are included in Table I.

In the absence of layer tilts, epitaxial layer RELPs lying on the asymmetric [**533**] reciprocal lattice vector are fully relaxed. Mathematical analysis of the first $InP_{0.85}As_{0.15}$ and second $InP_{0.73}As_{0.27}$ buffer layer RELPs reveal that these layers are 95 ± 5% relaxed and have total misfit strain values of ε_{misfit} = +0.54% and +0.87% respectively, with respect to the InP substrate. The degree of relaxation is consistent with their layer thickness being in excess of the critical thickness for these misfit values. The uppermost $InP_{0.68}As_{0.32}$ buffer layer's tilt-corrected RELP, peak number (4), neither lies near the [**533**] vector nor does it share the same b_{033} value as for the underlying second $InP_{0.73}As_{0.27}$ buffer layer RELP. Analysis shows that the third $InP_{0.68}As_{0.32}$ buffer layer is partially strained, calculated to be ~50 ± 10% relaxed with a total misfit strain of ε_{misfit} = +1.05% with respect to the InP substrate . While the third $InP_{0.68}As_{0.32}$ buffer is also above its critical thickness for relaxation, its relative misfit of $\Delta\varepsilon_{misfit}$ = +0.18% with respect to its underlying $InP_{0.73}As_{0.27}$ layer is smaller than the relative misfits between $InP_{0.85}As_{0.15}$ and InP ($\Delta\varepsilon_{misfit}$ = +0.54%) and $InP_{0.73}As_{0.27}$ and $InP_{0.85}As_{0.15}$ ($\Delta\varepsilon_{misfit}$ = +0.33%). The smaller relative misfit between $InP_{0.68}As_{0.32}$ and its preceding $InP_{0.73}As_{0.27}$ layer may be the driver behind the incomplete relaxation. The active $In_{0.67}Ga_{0.33}As$ layer RELP lies directly above the third $InP_{0.68}As_{0.32}$ buffer, thus the in-plane lattice constant of the active $In_{0.67}Ga_{0.33}As$ TPV layer is coherent with the uppermost buffer layer, consistent with its small relative misfit of $\Delta\varepsilon_{misfit}$ = -0.05% with respect to the $InP_{0.68}As_{0.32}$ buffer. These measurements were repeated with the incident x-ray beam parallel to four orthogonal <011> crystal directions and within the experimental error the *average* relaxation of the $InP_{1-y}As_y$ buffers and

$In_{0.67}Ga_{0.33}As$ layer were found to be isotropic. However the rocking-curve $FWHM_{004}$ of the $In_{0.67}Ga_{0.33}As$ RELP varied periodically from a minimum value of ~250asec along [011] and [01$\bar{1}$] directions to ~400asec along [01$\bar{1}$] and [0$\bar{1}$1] directions, where the anisotropy in the RELP $FWHM_{004}$ might be associated with the different core structures and/or dislocation formation kinetics associated with α and β dislocations in the LMM layer structure [5,7].

(b) Crystallographic Layer Tilt and Anisotropic $In_{0.67}Ga_{0.33}As$ RELP Broadening

Crystallographic planes of heteroepitaxial layers generally exhibit a net average tilt relative to the substrate planes, where the tilt angle Ω_{tilt}^{layer} measured by HRXRD will vary sinusoidally as a function of sample azimuthal angle [5,13]. The relative layer tilt projected along the [011] crystalline directions was previously accounted for when determining the lattice parameters from the RSMs shown in Figs 2 and 3. Figure 4 shows the sinusoidal variation of measured layer tilt relative to the InP crystal planes, Ω_{tilt}^{layer}, as a function of sample azimuthal angle for the three $InP_{1-y}As_y$ buffer layers and $In_{0.67}Ga_{0.33}As$ active region (right hand axis). The left hand axis and diamond-markers shows the sinusoidal dependence of InP substrate crystallographic tilt relative to the sample surface due to the intentional 2° misorientation of the (100) planes from the substrate surface towards [1$\bar{1}$0]. The magnitude of the substrate misorientation and the epitaxial layer tilts were found from the amplitude of the least squares fit of the data to a sine function. The measurements demonstrate that the substrate misorientation is indeed 2° from the surface normal. The first $InP_{0.85}As_{0.15}$ buffer is tilted ~0.05° away from the InP substrate inclination towards the substrate normal and the second $InP_{0.73}As_{0.27}$ buffer is also tilted away from the substrate inclination but by a larger tilt angle of 0.17°. These values are within the expected range of tilts predicted for the relief of compressive strain in lattice mismatched epitaxy [13]. The second $InP_{0.73}As_{0.27}$, the third $InP_{0.67}As_{0.337}$ buffer and the active $In_{0.67}Ga_{0.33}As$ layers all share the equivalent tilt relative to the InP substrate, where it is important to note that the uppermost two epilayers exhibit no net tilt with respect to the preceding second $InP_{0.73}As_{0.27}$ buffer layer. In the previous section the first and second $InP_{1-y}As_y$ buffers were found to be nearly fully relaxed due to the efficient relief of the relative misfit strains of $\Delta\varepsilon_{misfit}$ = +0.54% and +0.33% in these layers. As discussed in reference [13], layer tilt in non-pseudomorphic heteroepitaxial growth on vicinal substrate's is a result of strain relaxation due to

an asymmetry in the slip systems and/or preferential glide of certain types sets of dislocation types to accommodate the strain relaxation. The third $InP_{0.67}As_{0.33}$ buffer has a much smaller relative misfit strain of $\Delta\varepsilon_{misfit} = +0.18\%$ which results in partial relaxation of the strained layer however unlike the preceding two buffer layers, tilt does not play an appreciable role in the relaxation process. The absence of any net layer tilt relative to its preceding layer indicates that the density and/or dynamics of misfit dislocations at this $InP_{0.73}As_{0.27}/InP_{0.67}As_{0.33}$ interface is appreciably different than for the previous two layers. The absence of any measurable layer tilt and relaxation in the $In_{0.67}Ga_{0.33}As$ relative to the preceding final $InP_{0.67}As_{0.33}$ layer is consistent with the coherent heteroepitaxial growth of two nearly lattice matched materials.

A sinusoidal variation of the $In_{0.67}Ga_{0.33}As$ rocking curve $FWHM_{400}$ vs. azimuthal angle is observed (shown also in Fig 4). The minimum $FWHM_{400}$ of ~250asec is observed along [011] and $[0\bar{1}1]$ directions and the maximum $FWHM_{400}$ of ~400asec is observed along the $[01\bar{1}]$ and $[0\bar{1}1]$ directions. An average value of $FWHM_{avg}$ of 330asec is obtained when the rocking curve widths were averaged for 8 equally spaced sample azimuths. Despite the lack of an observable net average layer tilt in the uppermost $InP_{0.67}As_{0.33}$ and $In_{0.67}Ga_{0.33}As$ epitaxial layers relative to the fully relaxed $InP_{0.73}As_{0.27}$ buffer, the observed asymmetry in the $In_{0.67}Ga_{0.33}As$ RELP $FWHM_{400}$ with respect to the group III and group V crystalline faces suggests that there is in fact an anisotropy in the overall densities/distibutions of α and β type dislocations which influences the crystalline structure in the active TPV layer.

6.0 TPV diode photovoltaic performance and minority carrier recombination vs. x-ray rocking curve FWHM and diode surface morphology

0.74eV $In_{0.53}Ga_{0.47}As$ n/p junction diodes were tested and exhibited good 300K photovoltaic and spectral response under illumination. Under light generated current density of $2A/cm^2$ the cell open circuit voltage was V_{OC}=510mV with a Fill Factor of FF=75%, values that are consistent with best reported for 0.74eV bandgap TPV material [14]. The electrical figure of merit that is most sensitive to overall electronic material quality of the epitaxial material is the open circuit voltage, which we normalize to the bandgap (V_{OC}/E_{gap}) for comparison purposes. The excellent photovoltaic response of this lattice matched TPV n/p junction diode is consistent the high degree of crystalline perfection inferred from Fig. 1 which indicates coherent epitaxial

growth of the diode layers. Table I includes the results of the triple axis RSM analysis, the normalized open circuit voltage, and the fill factor of these LM $In_{0.53}Ga_{0.47}As$ TPV devices.

0.6eV $In_{0.67}Ga_{0.33}As$ n/p junction diodes grown on semi-insulating (SI) InP having heavily doped tellurium $InP_{1-y}As_y$ buffers[1,9] exhibit good 300K photovoltaic response under illumination and TPV energy conversion efficiency in excess of 20%. Under light generated current density of $2A/cm^2$ the 300K n/p junction open circuit voltage was V_{OC}=405mV with a Fill Factor of FF=72% as listed in Table I. Despite the order of magnitude larger x-ray rocking curve $FWHM_{400}$ of the LMM 0.6eV $In_{0.67}Ga_{0.33}As$ layer RELP compared to the LM 0.74eV $In_{0.53}Ga_{0.47}As$ layer RELP ($330asec_{average}$ vs. 30asec), the normalized open circuit voltage (V_{OC}/E_{gap}) is only slightly less than for the LM 0.74eV diodes. Therefore we conclude that the misfit-related dislocations present in the optimized 0.6eV LMM $In_{0.67}Ga_{0.33}As$ TPV epitaxial layers are not dominating the photovoltaic response compared with the intrinsic minority carrier recombination processes due to Auger and radiative processes and the native point defects (e.g. vacancies, interstitials, impurities) that would be present both in both lattice matched and lattice mismatched material $In_yGa_{1-y}As$.

To date, the optimal electrical performance from LMM 0.6eV $In_{0.67}Ga_{0.33}As$ TPV diodes have been grown on SI InP substrates and have high tellurium doping in the $InP_{1-x}A_x$ buffer layers. LMM 0.6eV $In_{0.67}Ga_{0.33}As$ TPV diode material has been synthesized under equivalent MOVPE growth conditions except having: (1) zinc-doped $InP_{1-x}A_x$ buffers, (2) undoped $InP_{1-x}A_x$ buffer layers and (3) heavily doped tellurium $InP_{1-x}A_x$ buffers grown on n-type conducting InP substrates. These variations in buffer layer doping and substrate type resulted in significant $In_{0.67}Ga_{0.33}As$ RELP broadening along the <011> directions, rougher surface morphology, and degradations in electrical performance despite keeping all other growth conditions (growth rate, III/V ratio, growth temperature …) equivalent. Figure 5 shows the (**400**) triple-axis rocking curve from (Curve A) LM 0.74eV $In_{0.53}Ga_{0.47}As$ TPV epitaxial layer and (Curves B,C,D) from LMM 0.6eV $In_{0.67}Ga_{0.33}As$ TPV epitaxial layers representing the full range of $In_yGa_{1-y}As$ rocking curve $FWHM_{004}$ measured during this investigation. As observed previously in the RSMs of Figs 1 and 2, the optimized LMM 0.6eV $In_{0.67}Ga_{0.33}As$ TPV diodes grown on tellurium doped $InP_{1-y}As_y$ 3-step buffers on SI InP substrates (curve B) has order of magnitude larger rocking-curve $FWHM_{400}$ than the LM $In_{0.53}Ga_{0.47}As$ TPV diodes. Curves C and D are rocking curves from 0.6eV $In_{0.67}Ga_{0.33}As$ TPV diodes grown with zinc doped $InP_{1-y}As_y$ 3-step buffers that were

found to exhibit degraded photovoltaic response. Severe broadening of the $In_{0.67}Ga_{0.33}As$ RELP rocking curve ($FWHM_{400}$ > 600arcsec) corresponded to the lowest performing TPV diodes. The degradation in photovoltaic response was primarily due to the sample open circuit voltage.

Figure 6 plots the dependence of the normalized open circuit voltage (V_{OC}/E_{gap}) vs. the rocking curve $FWHM_{400}$ for LM $In_{0.53}Ga_{0.47}As$ and the series of LMM $In_{0.67}Ga_{0.33}As$ TPV diodes grown under equivalent conditions except varying the $InP_{1-y}As_y$ buffer dopants and InP substrate type. As previously stated, the V_{OC}/E_{gap} from optimal LMM $In_{0.67}Ga_{0.33}As$ epitaxial diode material approaches that of the lattice matched diode material, indicating that optimized buffer layers can enable similar electronic material quality as for lattice matched $In_yGa_{1-y}As$. However, upon deterioration of the LMM crystalline quality in non-optimized epitaxial layer structures (where the deterioration of crystalline quality is inferred from the increase in rocking curve $FWHM_{400}$) a rapid decrease in V_{OC}/E_{gap} is measured.

Open circuit voltage degradation in crystalline photovoltaic materials often results from a reduction in minority carrier lifetime due to the presence of electrically active crystalline defects. Figure 7 shows two transient photoluminescence (TRPL) response curves used to measure minority carrier lifetime from p-type double heterostructure (DH) samples [15,16]. The DH samples were LMM $In_{0.67}Ga_{0.33}As$ epitaxial layers having front and back $InP_{0.68}As_{032}$ minority carrier confinement layers. The first decay curve is that from a DH sample grown on tellurium doped 3-step $InP_{1-x}As_x$ buffers; the second decay curve is that from a DH sample grown on undoped $InP_{1-x}As_x$ 3-step buffers. Both DH samples were grown under otherwise equivalent conditions on SI 2° misoriented (100) InP substrates. The measured x-ray RELP positions indicate equivalent values of average layer strain and composition for all layers in both samples. The initial exponential TRPL decay rate from both samples, corresponding to initial light injected electron densities in the range of mid $10^{15}cm^{-3}$, are equivalent and give a minority carrier lifetime of 134±3ns at those injection levels. At light injections levels less than $<< 10^{15}cm^{-3}$, the recombination rate in the DH sample having undoped $InP_{1-x}As_x$ buffers rapidly increases while the DH sample grown on tellurium doped $InP_{1-x}As_x$ maintains its constant exponential decay. The rapid low injection decay observed for the $In_{0.67}Ga_{0.33}As$ DH sample having undoped $InP_{1-x}As_x$ buffers has also been observed in AlGaAs/GaAs solar photovoltaic material and was attributed to the presence of electrically-active deep level defects resulting by non-optimal growth conditions [17]. Triple-axis rocking curves from the DH sample having

undoped $InP_{1-x}As_x$ buffer reveal that the $In_{0.67}Ga_{0.33}As$ RELP $FWHM_{400}$ is 350asec along [011] and has an average value of $FWHM_{avg}$ of 380asec when averaging over 45° azimuthal increments. For the DH sample having tellurium doped buffers, the $In_{0.67}Ga_{0.33}As$ RELP $FWHM_{400}$ was measured to be 250asec along [011] with average value $FWHM_{avg}$ = 330asec, consistent with those values measured in optimized TPV n/p junction diode layers grown on tellurium doped buffers. Thus, similar to open circuit voltage in LMM $In_{0.67}Ga_{0.33}As$ TPV diodes, we can correlate the degradation in electronic recombination dynamics in the LMM $In_{0.67}Ga_{0.33}As$ DH samples with broadening of the active layer RELP $FWHM_{400}$.

In addition to the RELP broadening in non-optimized epitaxial structures, a degradation in surface morphology was observed in the LMM $In_{0.67}Ga_{0.33}As$ samples exhibiting broader $FWHM_{400}$. Nomarski (200X) microscope images from the sample surfaces are shown in Fig 8 which corresponds to the same samples measured in the rocking curves B,C,D from Fig 5. The optimized LMM diode samples have tellurium doped buffers also exhibit the most specular surfaces and uniform cross hatch pattern illustrated in Fig. 8a. In contrast, non-optimized LMM diode samples with broadest $FWHM_{400}$, shown in Fig 8c, exhibits a non-uniform, rough surface, with heavily defected regions that are aligned along the [011] directions.

Previous studies have indicated that tellurium acts as a surfactant during growth, resulting in smoother surfaces [9]. These findings are consistent with the smooth surface morphologies shown in Fig. 8a and is a plausible explanation for the higher measured open circuit voltage, better minority carrier recombination characteristics, and narrower x-ray rocking curve $FWHM_{400}$ when incorporating tellurium doping in the buffer layers compared to $In_{0.67}Ga_{0.33}As$ material grown using undoped or zinc doped buffers. However, there is not a clear explanation why $In_{0.67}Ga_{0.33}As$ n/p junction diode performance might depend on the InP substrate's conductivity type: the only two differences between these experiments were (1) conducting n-type and p-type substrates contained an average etch pit density (EPD) of ~100cm^{-2}, while SI InP substrates contained an area of ~1000cm^{-2} and (2) substrate heater power required adjustments to maintain equivalent wafer surface temperature during growth on SI and conducting InP substrates leaving open the possibility of subtle differences in the growth temperature. While previous studies [18] reported that substrate dislocation density influenced the misfit dislocation kinetics and the density of epitaxial layers grown well above the critical

thickness, we observed no differences in average relaxation between these samples grown on low EPD InP substrates other than the broadening of the RELP along <011> directions.

7.0 Conclusions

Lattice-matched (LM) $In_{0.53}Ga_{0.47}As$ and lattice-mismatched (LMM) $In_{0.67}Ga_{0.33}As$ TPV diodes were grown by metal organic vapor phase epitaxy (MOVPE) and their structural characteristic were evaluated using triple axis x-ray diffraction measurements. Analysis of the relative positions of the reciprocal lattice point (RELP) maxima provide the strain, arsenic content, tilt magnitude/direction, and mosaicity of the epitaxial layers which comprise the TPV n/p junction diode structure. Significant misfit-related broadening of the x-ray rocking curve is present in the optimized LMM 0.6eV $In_{0.67}Ga_{0.33}As$ TPV epitaxial layers, however comparison of its electrical characteristics with the LM material indicates that the misfit-related imperfections in the $In_{0.67}Ga_{0.33}As$ are not dominating the photovoltaic response compared to the intrinsic minority carrier recombination processes due to Auger and radiative processes and the native point defects that would be present both in both LM and LMM $In_yGa_{1-y}As$. Additional broadening of the scattered x-ray intensity around the LMM $In_{0.67}Ga_{0.33}As$ RELP maximum correlates with degradations both in TPV diode open circuit voltage and minority carrier lifetime in non-optimized LMM material, showing that the triple axis x-ray technique is a useful characterization tool for evaluating electronic material quality of epitaxial TPV n/p junction diodes. Triple axis x-ray analysis of the LMM $In_{0.67}Ga_{0.33}As$ structures indicate that layer tilt plays an observable role in the relaxation process of the first two highly mismatched $InP_{1-y}As_y$ buffers, however tilt is not present in the uppermost $InP_{0.68}As_{0.32}$ buffer layer or active layer. However the periodicity in the $In_{0.67}Ga_{0.33}As$ rocking curve FWHM vs. azimuthal angle in the optimized structure are indicative that the misfit network remains "imperfect", having dissimilar densities/distributions of α and β dislocations.

Acknowledgements

The authors would like the thank T. Lavery and L. Danielson of Lockheed Martin and R. Huang of MIT Lincoln Laboratory for current-voltage measurements and M. Connors of MIT Lincoln Laboratory and G. Taylor of Sarnoff Corporation for device processing.

References

[1] B. Wernsman, R.R. Siergiej, S.D. Link, R.G. Mahorter, M.N. Palmisiano, R.J. Wehrer, R.W. Shultz, G.P. Schmuck, R.L. Messham, S. Murray, C.S. Murray, F. Newman, D. Taylor, D.M. Depoy, and T. Rahmlow, in IEEE Trans. on Electron Devices, 51, (2400), 512-515.

[2] Harold J. Hovel in Semiconductors and Semimetals Volume 11, Ed. R.K. Willardson and A.C. Beer (Academic Press Inc., Orlando 1975).

[3] Paul F. Fewster, Reciprocal Space Mapping in Critical Reviews in Solid State and Materials Sciences, 22, (1997) 69-110.

[4] Guenther Bauer, Jianhua Li, Ewald Koppensteiner, J. Crytsal Growth, 157 (1995) 61-67.

[5] J.A. Olsen, E.L. Hu, S.R. Lee, I.J. Fritz, A.J. Howard, B.E. Hammons, and J.Y. Tsao, J. Appl. Phys. 79 (1996) 3578-3584.

[6] M.K. Hudait, Y. Lin, D.M. Wilt, J.S. Speck, C.A. Tivarus, E.R. Heller, J.P Pelz, S.A. Ringel, Appl. Phys. Lett., 82 (2003) 3212-3214.

[7] M.K. Hudait, Y. Lin, M.N. Palmisiano, C.A. Tivarus, J.P Pelz, and S.A. Ringel, J. Appl. Phys. 95 (2004) 3952-3960.

[8] S. L. Murray, F.D. Newman, C.S. Murray, D.M Wilt, M.W. Wanlass, P. Ahrenkiel, R. Messham, and R.R. Siergiej, Semiconductor Science and Technology, 18, (2003) S202-208.

[9] F.D. Newman, M.A. Stan, S.L. Murray, C.S. Murray, J. Crystal Growth, 272 (2400) 650-657.

[10] David Wilt, Rebecca Wehrer, Marc Palmisiano, Mark Wanlass, and Christopher Murray, Semiconductor Science and Technology, 18, (2003) S209-215.

[11] A. Krost, G. Bauer, and J. Woitok in Optical Characterization of Epitaxial Semiconductor Layers, Eds. G. Bauer and W. Richter (Springer, Berlin 1996) 351-352.

[12] M. Fatemi and R.E. Stahlbush, Appl. Phys. Lett., 58, (1991) 825-827.

[13] J.E. Ayers, S.K. Ghandi, and L.J. Schowalter, J. Crystal Growth, 113, (1991) 430-440.

[14] M.K. Hudait, C.L. Andre, O. Kwon, M.N. Palmisiano, and S.A. Ringel, IEEE Elect. Dev. Lett., 23 (2002) 697-699.

[15] S. Anikeev, D. Donetski, G. Belenki, S. Luryi, C.A. Wang, J.M. Borrego, G. Nichols, Appl. Phys. Lett., 83 (2003) 3317-3319

[16] D. Donetski, , S. Anikeev, G. Belenky, S. Luryi, C.A. Wang, G. Nichols, Appl. Phys. Lett., 81, (2002) 4769-4771.

[17] R. K. Ahrenkiel, J. Appl. Phys. Vol. 62, no. 7, pp. 2937-2941 (1987).

[18] J.F. Klern, W.S. Fu, P.L. Gourley, E.D. Jones, T.M. Brennan, and J.A. Lott, Appl. Phys. Lett., 56, (1990) 1350-1352.

Table I. Lattice parameters for MOVPE grown LM 0.74eV and LMM 0.6eV $InGa_{1-y}As_y$ TPV diodes

TPV Diode Structure	Epitaxial Layer	a_n (nm)	a_p (nm)	a_{relax} (nm)[a]	Relaxation[b]	InAs content[a]	(400) FWHM (arcsec)	Normalized V_{OC}/E_{gap}[c]	Fill Factor (FF)
LMM 0.6eV InGaAs	$InP_{1-x}As_x$ buffer 1	0.5898	0.5898	0.5898	~ 97%	x=*0.15*	-		
	$InP_{1-x}As_x$ buffer 2	0.5920	0.5917	0.5918	~ 95%	x=*0.27*	-		
	$InP_{1-x}As_x$ buffer 3	0.5934	0.5924	0.5929	~ 50%	x=*0.32*	-		
	$In_yGa_{1-y}As$ active	0.5928	0.5925	0.5926	~ 0%	*y=0.67*	*250 min. 330 avg.*	*0.67*	*72%*
LM 0.74eV InGaAs	$In_yGa_{1-y}As$ active	0.5871	0.5869	0.5870	~ 0%	*y=0.53*	*30 min 30 avg.*	*0.69*	*75%*

[a] The relaxed lattice constant of each epitaxial layer is found from: $a_{relax} = [2\nu \cdot a_p - a_n(\nu-1)] / (1+\nu)$ where $\nu = C_{12}/(C_{11}+C_{12})$ is the Poisson ratio calculated from an interpolation (Vegard's Law) of its binary values [12] ($\nu_{InP}=0.357$, $\nu_{InAs}=0.352$, $\nu_{GaAs}=0.311$). The arsenic content is then calculated from a_{relax} by interpolating between binary lattice constants $a_{InP}=0.58688$nm, $a_{InAs}=0.60583$nm, $a_{GaAs}=0.56533$nm. .

[b] Relaxation of an epitaxial layer (i) is defined with respect to the in-plane lattice constant of the underlying substrate/epitaxial layer (i-1): $100 \times (a_p^{\,i}-a_p^{\,i-1}) / (a_{relax}^{\,i}-a_p^{\,i-1})$

[c] The normalized open circuit voltage V_{OC}/E_{gap} is defined as the measured open circuit voltage at 300K under light generated current densities of $2A/cm^2$ divided by the $InGa_{1-y}As_y$ bandgap.

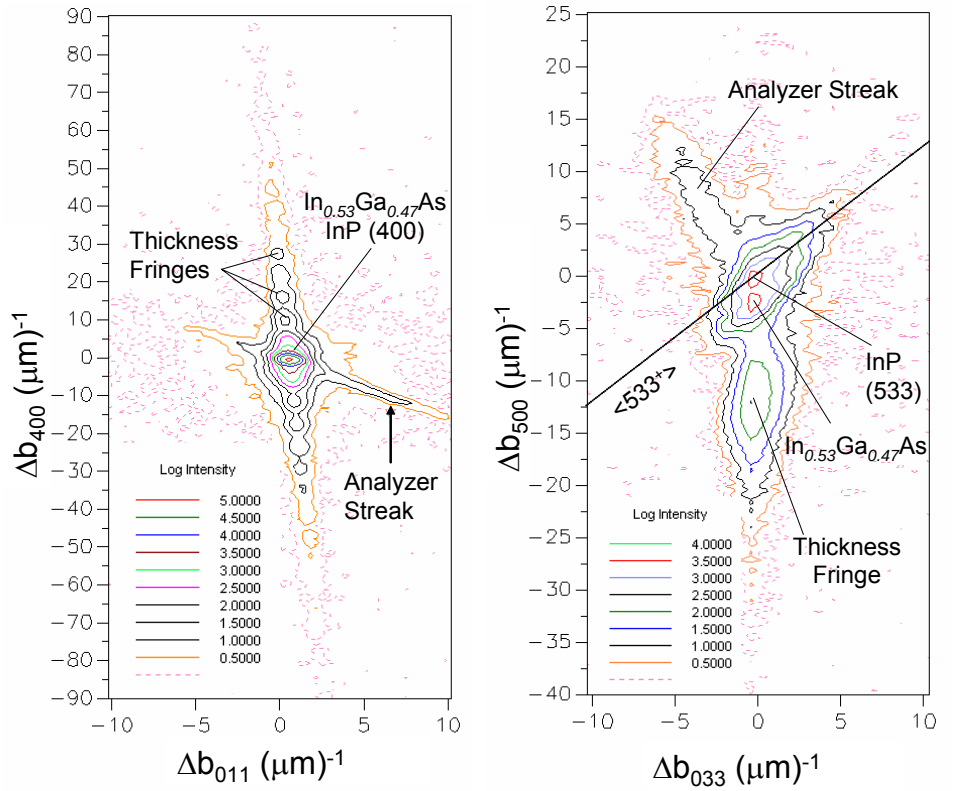

(a) (b)

Figure 1 (a) Measured (**400**) and (b) glancing exit (**533**) triple-axis RSM of 0.74eV lattice matched $In_{0.53}Ga_{0.47}As$ TPV diode. Iso-intensity contours are plotted in logarithmic (counts per second) – scales are included in each figure.

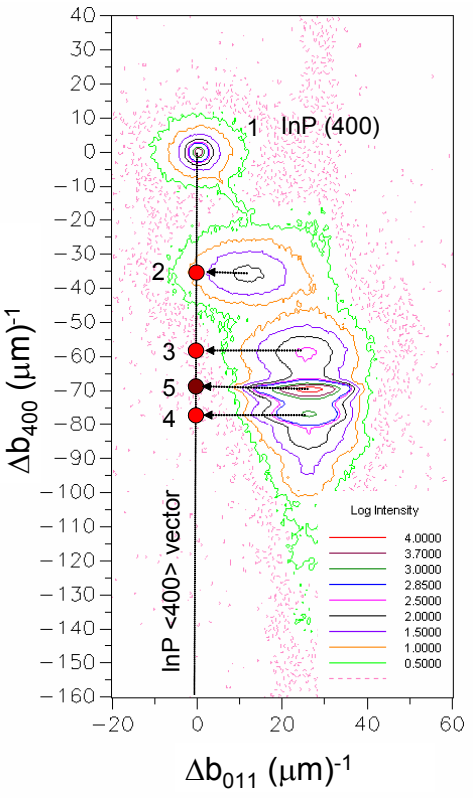

Figure 2. Measured symmetric (**400**) triple-axis RSM of 0.60eV LMM $In_{0.67}Ga_{0.33}As$ TPV diode. The incident x-ray beam was parallel to the plane containing the [100] and [011] crystallographic directions. RSM diffraction peak assignments correspond to InP substrate (1), the first $InP_{0.85}As_{0.15}$ buffer layer (2), the second $InP_{0.72}As_{0.27}$ buffer layer (3), the third $InP_{0.68}As_{0.32}$ buffer layer (4), and the 0.6eV $In_{0.67}Ga_{0.33}As$ active region (5). The shift in the measured layer RELPs along Q_{110} is due to crystallographic tilt between the layers and the InP substrate. Rotating each RELP about the (000) origin and projecting them onto the (400) reciprocal lattice vector, as shown by the filled circles, determines the angles that the asymmetric RELPs must be rotated in order to perform the strain analysis.

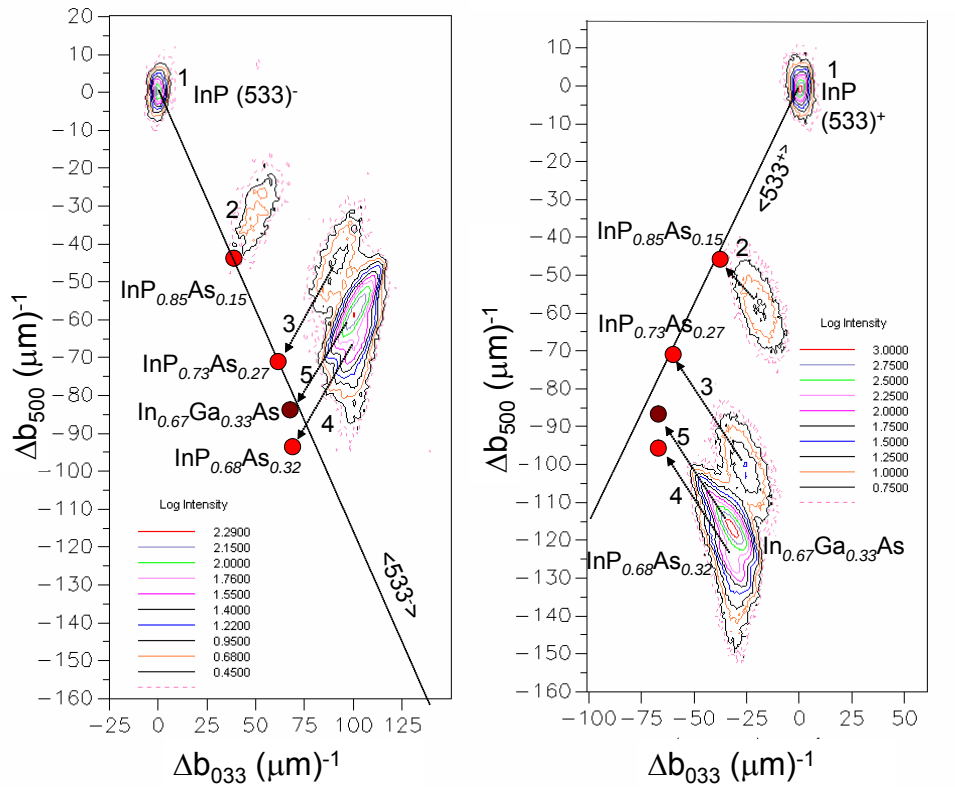

Figure 3. Asymmetric glancing-incidence and glancing-exit RSMs about the (**533**) RELPs from optimized 0.60eV LMM $In_{0.67}Ga_{0.33}As$ TPV diode. The incident x-ray beam was parallel to the plane containing the [100] and [011] crystallographic directions. The relative tilt angle of each layer determined from Figure 2 is used to tilt-correct each the asymmetric diffraction peaks for the strain analysis. The tilt corrected RELPs are shown as the filled circles in each figure and the in-plane and out-of-plane lattice constants and layer relaxation are then determined from these points.

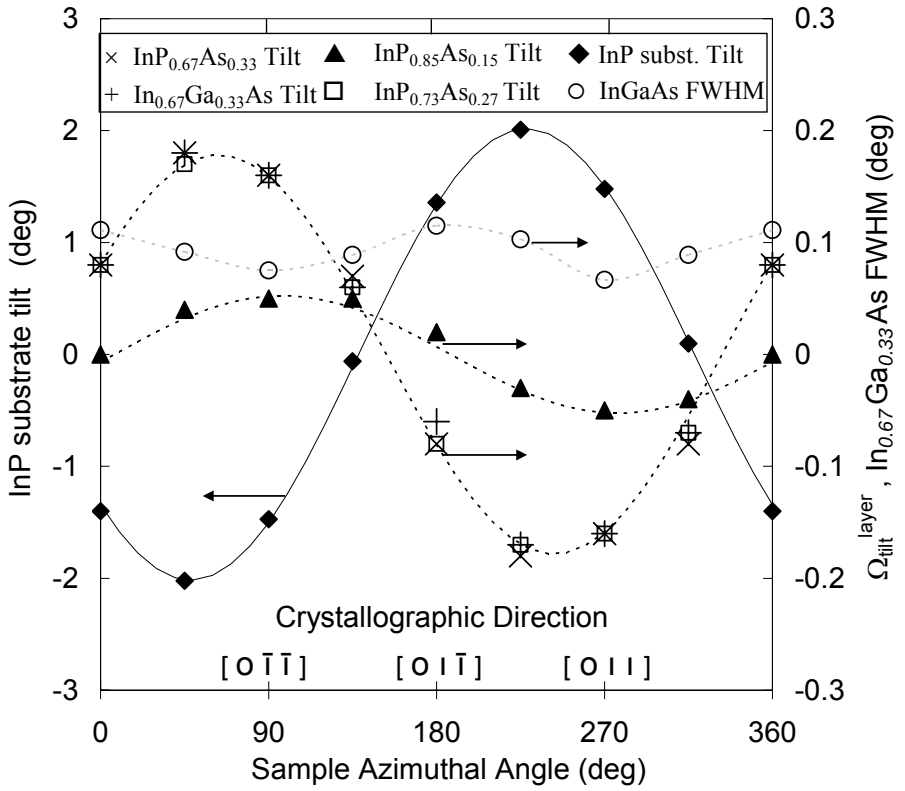

Figure 4. Crystallographic tilt of the first $InP_{0.85}As_{0.15}$, $InP_{0.73}As_{0.27}$, $InP_{0.68}As_{0.32}$ buffers, and $In_{0.67}Ga_{0.33}As$ active with respect to the InP crystal planes vs. wafer azimuthal orientation (right hand axis). The sinusoidal variation of InP crystallographic tilt with respect to the substrate surface is also shown in the figure to illustrate the direction and magnitude of the intentional 2° misorientation (left hand axis). The dependence of the active $In_{0.67}Ga_{0.33}As$ triple-axis rocking curve's full width at half maximum (FWHM) vs. sample azimuth is shown.

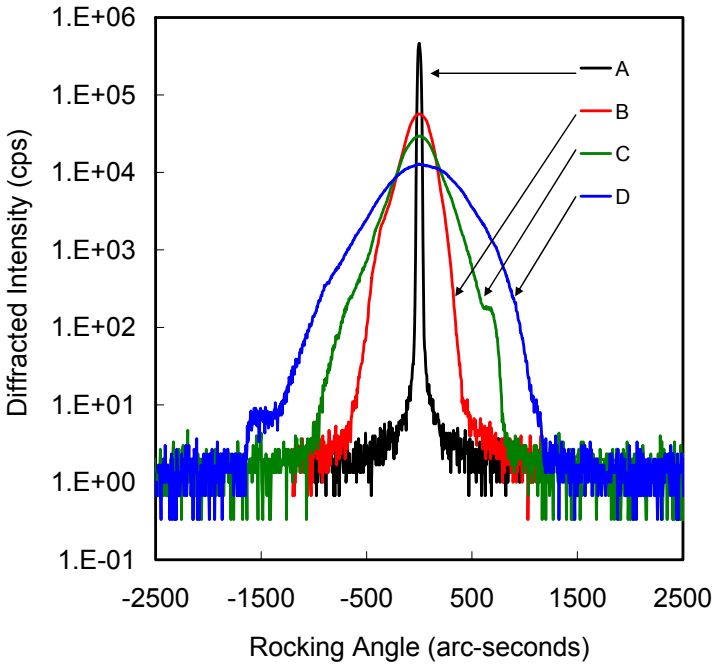

Figure 5. A. (**400**) triple-axis rocking curves from: (A) LM $In_{0.53}Ga_{0.47}As$ TPV active layer, (B) state of the art $In_{0.67}Ga_{0.33}As$ TPV diode active layer representative of >20% efficient TPV diode material [1], (C) $In_{0.67}Ga_{0.33}As$ TPV active layers exhibiting approximately 10% degradation in power output due to non-optimal growth conditions and (D) $In_{0.67}Ga_{0.33}As$ TPV diode material exhibiting 35% degradation due to non-optimal growth conditions.

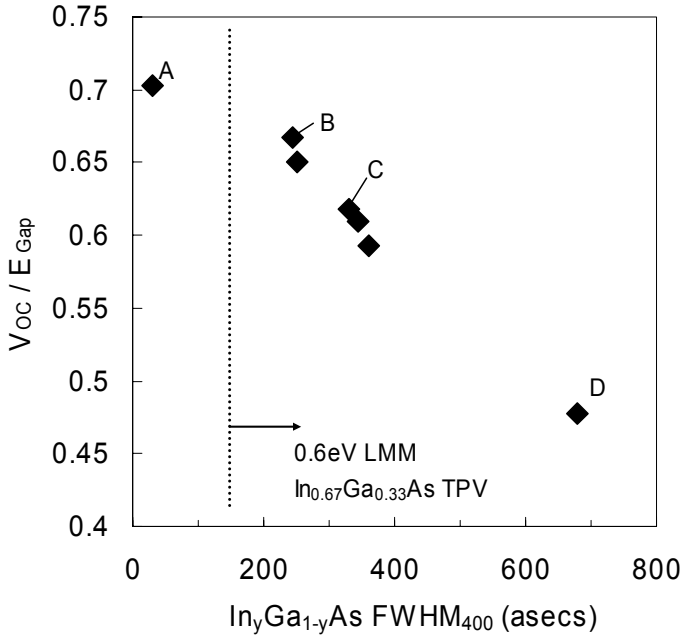

Figure 6. Measured values of normalized open circuit voltage (V_{OC}/E_{gap}) vs. $In_yGa_{1-y}As$ rocking curve $FWHM_{400}$. V_{OC} and E_{gap} were measured at 300K and all samples were measured under light generated current densities of $2A/cm^2$. The $FWHM_{400}$ from the rocking curves shown in Fig. 5 are labeled in this figure.

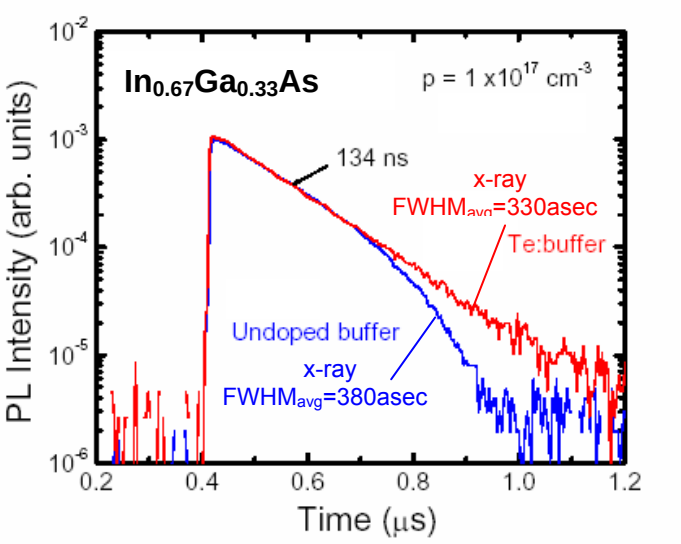

Figure 7. Transient photoluminescence (TRPL) decay curves from p-type LMM 0.6eV $In_{0.67}Ga_{0.33}As$ double heterostructure (DH) samples grown on tellurium doped and undoped step graded $InP_{1-y}As_y$ buffer layers. A rapid low injection TRPL decay rate and broader x-ray FWHM indicate a greater number of crystalline imperfections in the $In_{0.67}Ga_{0.33}As$ DH grown on undoped $In_yP_{1-y}As$.

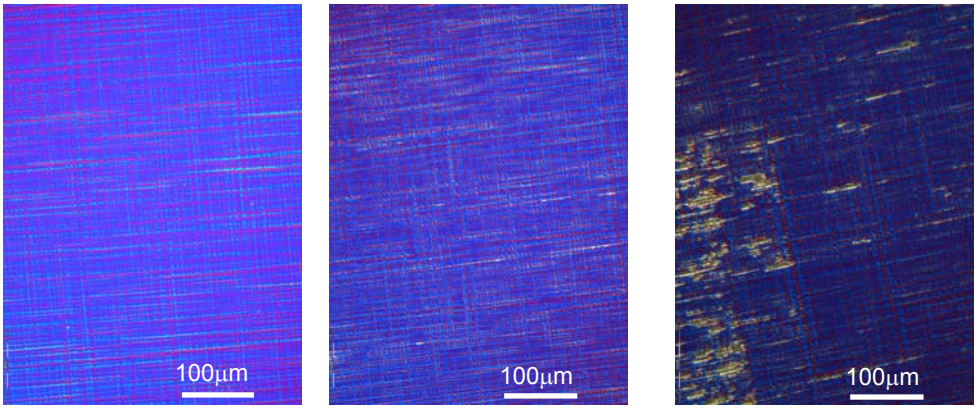

Rocking Curve B (8a) | Rocking Curve C (8b) | Rocking Curve D (8c)

Figure 8. Nomarski images of the LMM $In_{0.67}Ga_{0.33}As$ samples corresponding rocking curves B, C, and D shown Fig 5.